

THE ANNUAL CYCLE OF SURFACE RADIATION BUDGET OVER EUROPE

Pamela E. Mlynczak¹, G. Louis Smith² and Rainer Hollmann³

1. Science Systems and Applications, Inc., Hampton, Virginia, US

2. National Institute for Aerospace, Hampton, Virginia, US

3. German Meteorological Service, Offenbach, Germany

1. INTRODUCTION

Weather and climate are closely related to the radiation budget at the surface. A consortium of six European meteorological services together with EUMETSAT has established the Climate Monitoring Satellite Application Facility (CM-SAF) to develop and generate data sets for several key climate parameters, based on satellite data. The geophysical products range from data sets for radiation budget at the surface and at the top of the atmosphere, and they include cloud properties, water vapor content and profiles as well as temperature profiles. The derived CM-SAF data sets include daily and monthly-mean values of these surface fluxes at a resolution of 15 x 15 km². The surface radiation budget data sets include surface incoming shortwave radiation (SIS), surface albedo (SAL), surface downward longwave (SDL) and outgoing longwave radiation (SOL). Beside the global coverage of the water vapor products, all other products are so far provided on a regional basis covering Europe and parts of Africa.

This paper presents a study of the annual cycle of surface radiation budget SRB over Europe using these monthly-mean values. A principal component analysis is used to extract the time-histories of the various radiation terms, with associated maps computed as empirical orthogonal functions.

2. DATA SET

For the surface radiation budget data set, CM-SAF uses mainly the Meteosat Second Generation satellite and for coverage at higher latitudes uses also NOAA and METOP satellite instruments. The incoming solar radiation is computed by use of SEVIRI and GERB (broadband radiometer) measurements. For longwave surface radiation components, additional input from numerical

weather prediction models (temperature and humidity profiles) is used. The outgoing longwave flux product is so far purely model-based because the surface temperature of the NWP model is used as input. The surface net shortwave radiation (SNS) is computed from the SIS and SAL, and the surface net longwave radiation (SNL) is computed from the SDL and SOL components. Currently the CM-SAF uses the German Meteorological Service numerical weather prediction model GME. Data for the one-year period from January 2006 through December 2006 is used in this paper. Beginning with May 2007, the full disk of Meteosat Second Generation is provided, giving full coverage of Africa.

A sinusoidal projection is used for maps presented in this paper. The ordinate is latitude from 30°N to 70°N. The Greenwich meridian is the vertical center line of the map, and the abscissa scale is longitude from 60°W to 60°E at 30°N. The length along a latitudinal circle is constant for the abscissa, so that the longitude in degrees scales as the cosine of latitude; thus the maps preserve area.

3. ANNUAL MEAN SURFACE RADIATION

The first step in examining the annual cycle of surface radiation is to consider the annual mean of the various components. Next, maps of the parameters' variability will be examined.

Figure 1a is a map of the annual mean surface incoming shortwave flux SIS. The insolation at the top of the atmosphere depends only on latitude, thus the longitudinal variations of SIS are due primarily to clouds, with small variations due to water vapor and ozone. Figure 1b shows the annual mean surface net shortwave flux SNS. This map differs from fig. 1a due to differences of the surface albedo, which is greatest between land and ocean; thus in this map the locations of the Mediterranean, Baltic and Black Seas are apparent.

Corresponding author address: G. Louis Smith,
Mail Stop 420, Langley Research Center, NASA,
Hampton, Virginia, 23681, e-mail:
george.l.smith@nasa.gov

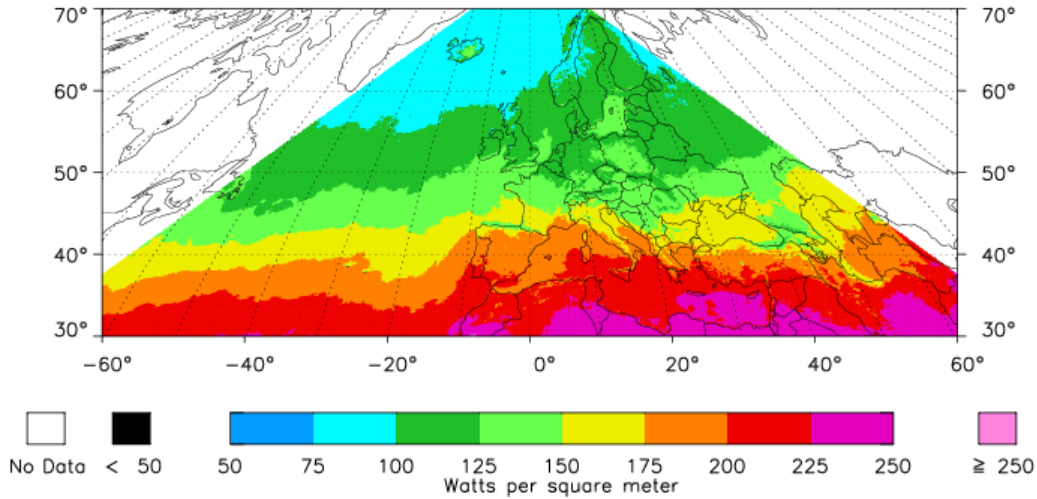


Figure 1a. Annual mean of surface incoming shortwave flux SIS in $W m^{-2}$.

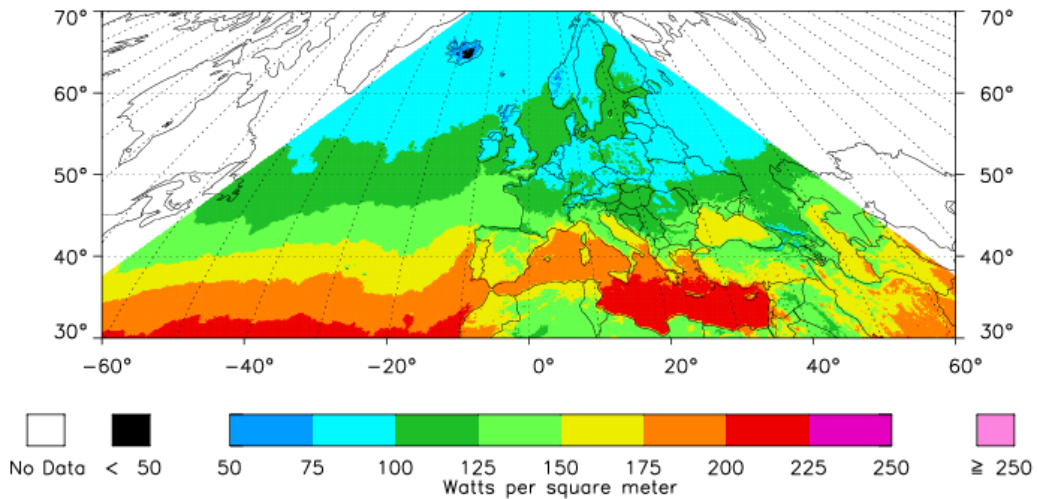


Figure 1b. Annual mean of surface net shortwave flux SNS in $W m^{-2}$.

Figure 2a shows the annual mean surface outgoing longwave flux SOL. SOL is a function only of temperature (emissivity is assumed to be 1.0), and the annual mean temperature is higher over ocean than over land or inland seas. Nevertheless, the Mediterranean, Baltic and Black Seas appear warmer than the surrounding lands. On the western side of the domain, the Labrador Current and Gulf Stream are clearly delineated. Over western and central Europe and northern Africa, the primary factor is latitude, but in the eastern part of the domain there are strong longitudinal variations.

Figure 2b shows the annual mean surface downward longwave flux SDL. Over the Atlantic Ocean south of approximately 45°N the SDL is

greater than $350 W m^{-2}$, but over land the SDL is less than $350 W m^{-2}$ from 30°N northward. Over much of the northeastern part of the domain SDL is less than $300 W m^{-2}$. It is speculated that there are more clouds over the ocean regions; hence, the SDL is greater than over land surfaces.

Figure 2c is a map of the surface net longwave flux SNL. North Africa, where the air is dry, has a large SNL cooling flux. With increasing latitude and decreasing temperatures, the reduced outgoing longwave SOL results in reduced SNL.

Figure 3 is a map of annual mean surface total net flux. This map is more zonal than the net longwave map, but there are large land-ocean differences.

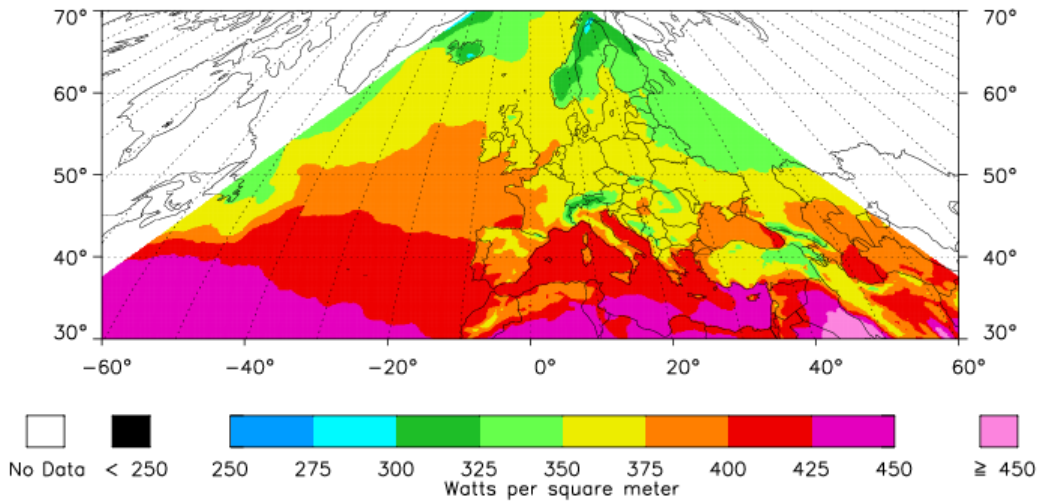


Figure 2a: Annual mean of surface outgoing longwave flux SOL in $W m^{-2}$.

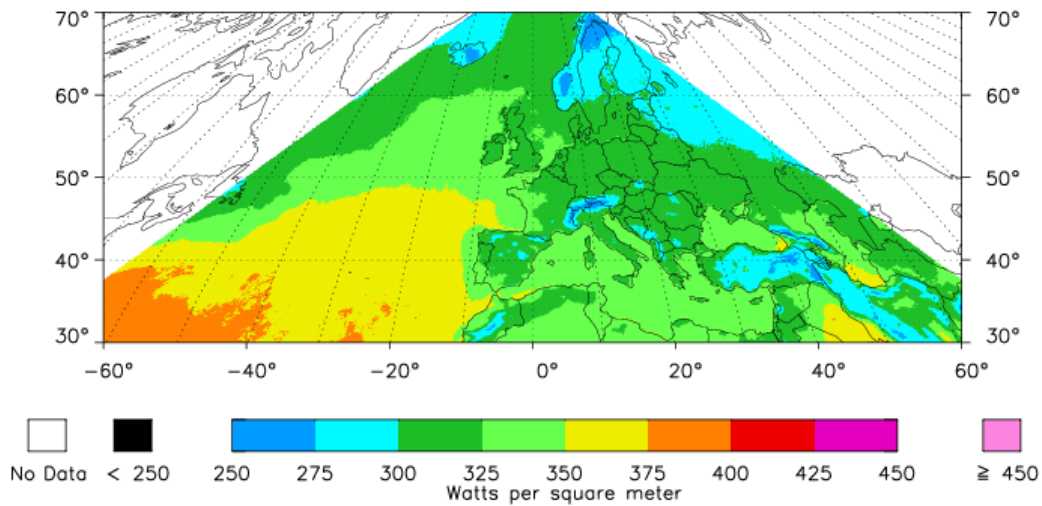


Figure 2b: Annual mean of surface downward longwave flux SDL in $W m^{-2}$.

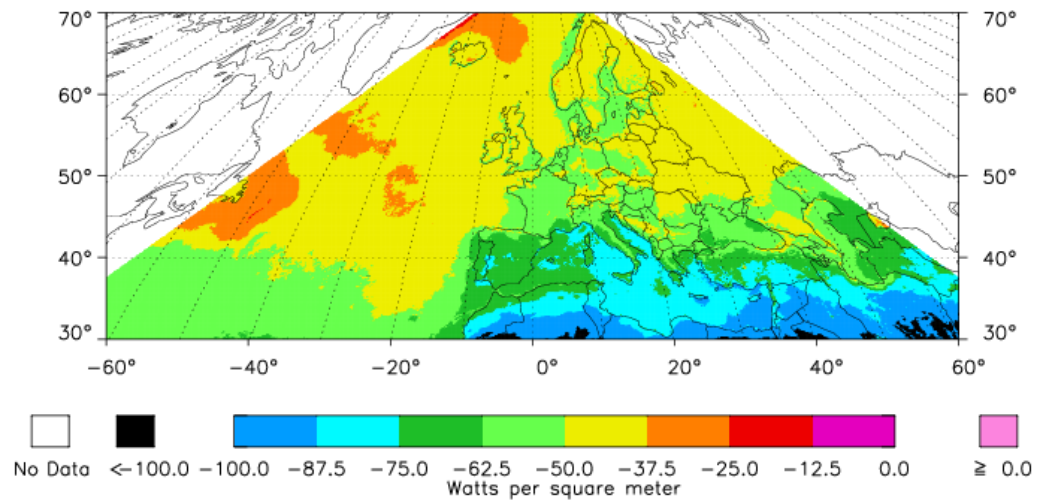


Figure 2c: Annual mean of surface net longwave flux SNL in $W m^{-2}$.

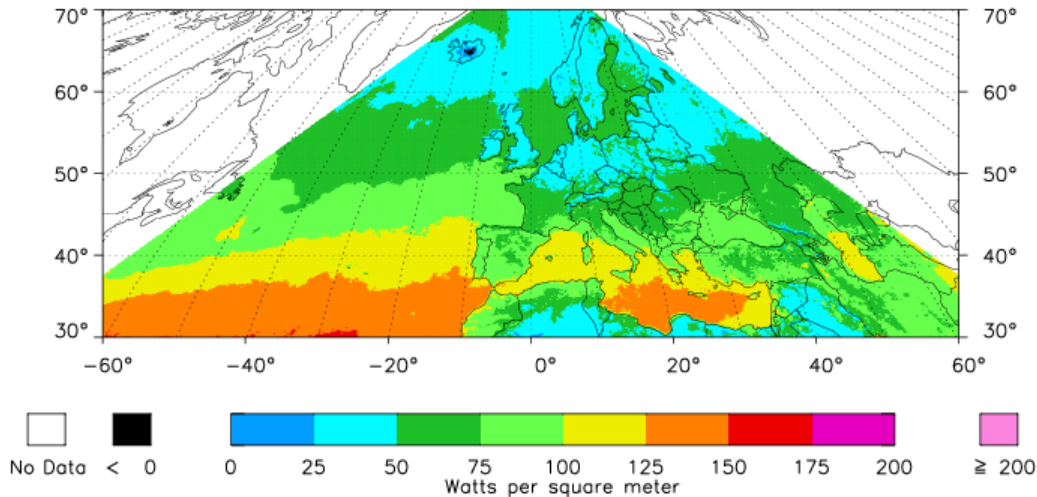


Figure 3: Annual mean of surface total net flux in W m^{-2} .

4. ANNUAL CYCLE OF SURFACE RADIATION

The annual cycle of a quantity for a given region is defined as the departure of the monthly mean values from the yearly mean value. The root-mean-square difference from this annual mean provides a useful measure of the variability of a quantity.

For the part of the domain which is covered by land, the area average RMS is listed in Table 1 for the various components of surface radiation. The SIS has the largest RMS variation, 52 W m^{-2} , followed by the SNS. The SOL has a variability of 32.2 W m^{-2} . SDL is coupled with SOL by boundary layer processes and has a smaller RMS, at 24.0 W m^{-2} . Also due to this coupling of the surface and lowest levels of air, the SNL has a variability of 10.0 W m^{-2} . Finally, because the SNS drives the SOL to which the SDL is coupled, the RMS of total net flux is 33.9 W m^{-2} , less than the SNS.

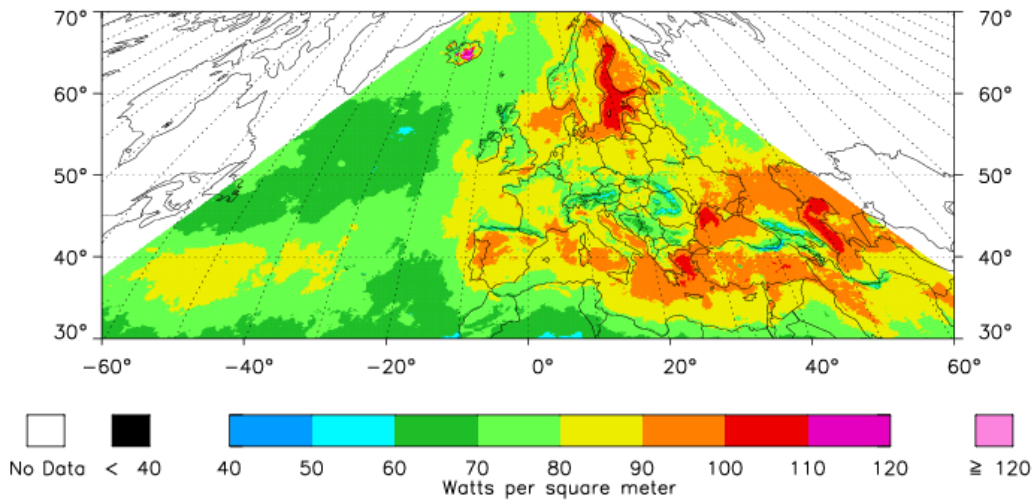
Figure 4 shows maps of RMS variation of SIS, SOL and SDL. The annual variability of SIS is less than 80 W m^{-2} over much of the ocean due to the nearly ubiquitous cloudiness. Over most of western and central Europe the SIS varies more than 80 W m^{-2} . The SOL shows variability of less than 20 W m^{-2} over the ocean and variability of 20 to 40 W m^{-2} for the inland seas and coastal regions of land. Further inland the variability is 40 to 70 W m^{-2} . The SDL has a similar pattern, with the RMS of SDL less than 20 W m^{-2} over most of the ocean and greater than 30 W m^{-2} for most of the land regions, exceeding 50 W m^{-2} in desert and steppe regions.

A principal component analysis has been applied to the seasonal cycle of the radiation components over the part of the domain which is land. The ocean has a large heat storage and small variability of temperature, thus its annual cycle of temperature will lag that of land and result in a mix which will require more terms to describe both parts of the domain. The first two normalized eigenvalues are listed in Table 1 for the SRB components over land. For all but SNL, the first principal component describes more than 90% of the variance, thus only the first PC and empirical orthogonal function EOF will be discussed here.

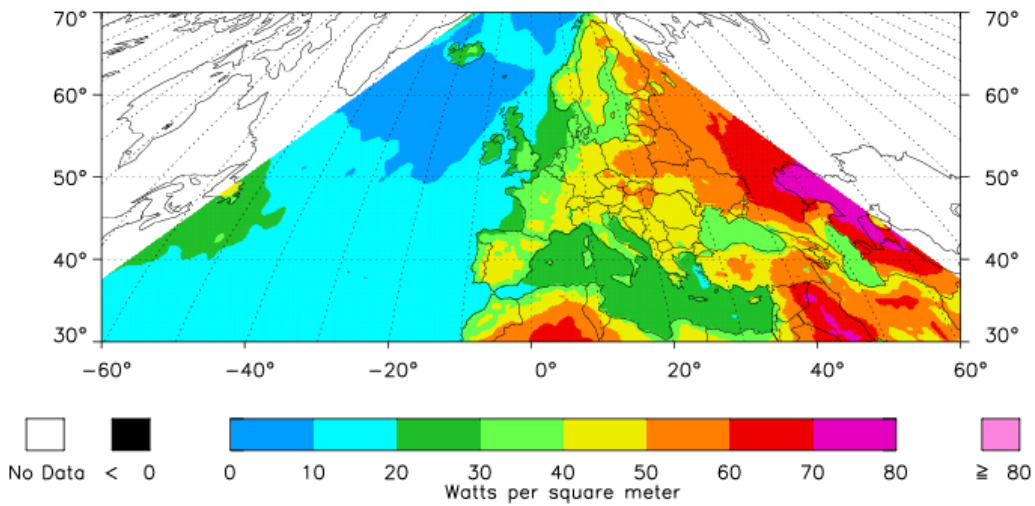
Figure 5 shows the first four PCs for incoming shortwave SIS. The average of a principal component is zero over the year, since the annual mean of SIS has been subtracted from the data to obtain the annual cycle. PC-1 has a peak of 76 W m^{-2} in June during the northern summer solstice and a minimum of -64 W m^{-2} in December during the northern winter solstice. This asymmetry of maximum and minimum deviates from a sine wave. This difference of the maximum and minimum is not explained by the annual cycle of insolation at the top of the atmosphere. The eccentricity of the Earth's orbit causes an annual sine variation in TOA insolation, with no asymmetry as seen here. It is conjectured that this is an effect of cloud variation. Additional research is needed here. The higher order PCs are fairly irregular and have small values, less than 4 W m^{-2} for most months.

Table 1: RMS variability of surface radiation components and normalized variances for first two EOFs over land.

| Quantity | | RMS, $W m^{-2}$ | EOF-1 | EOF-2 |
|-----------|----------------|-----------------|-------|-------|
| SIS | Shortwave Down | 52.0 | 0.962 | 0.013 |
| SNS | Shortwave Net | 41.7 | 0.954 | 0.017 |
| SOL | Longwave Up | 32.2 | 0.960 | 0.021 |
| SDL | Longwave Down | 24.0 | 0.915 | 0.041 |
| SNL | Longwave Net | 10.0 | 0.797 | 0.075 |
| Total Net | | 33.9 | 0.963 | 0.013 |

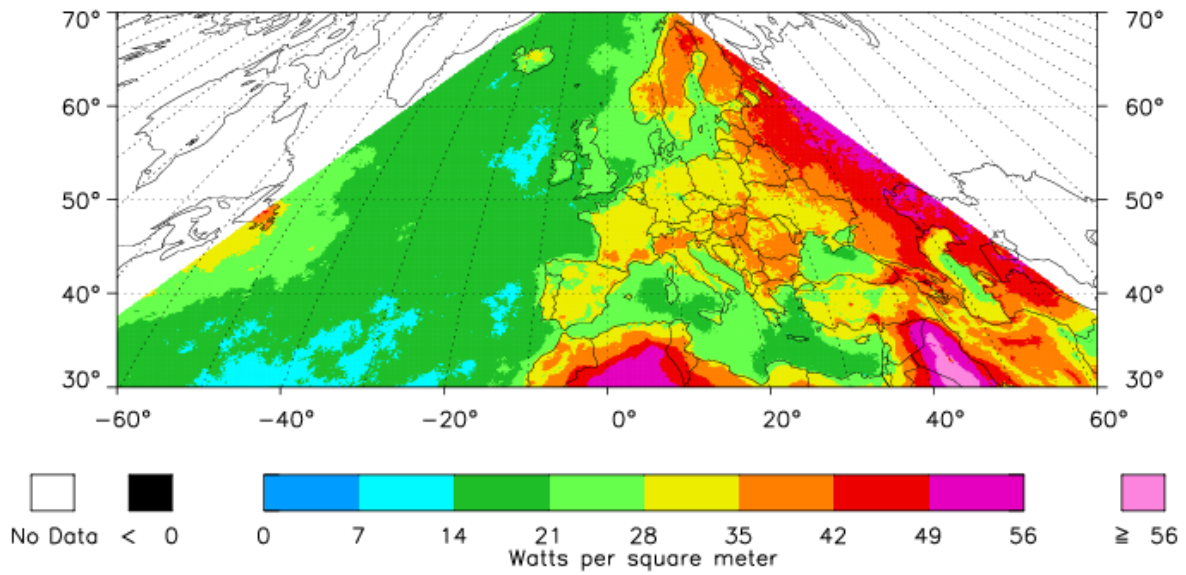


a. RMS of surface incoming shortwave flux SIS in $W m^{-2}$.



b. RMS of surface outgoing longwave flux SOL in $W m^{-2}$.

Figure 4: Annual RMS variability of surface incoming shortwave, outgoing longwave and downward longwave fluxes (continued).



c. RMS of surface downward longwave flux SDL in $W m^{-2}$.

Figure 4: Annual RMS variability of surface incoming shortwave, outgoing longwave and downward longwave fluxes (concluded).

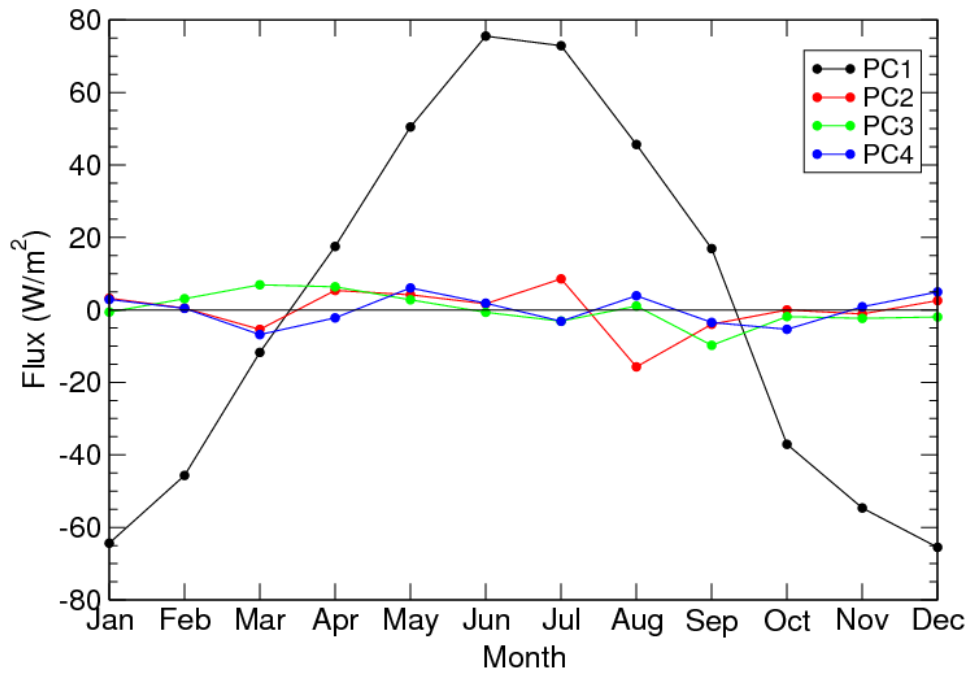


Figure 5: Principal components of the annual cycle of surface incoming shortwave flux SIS.

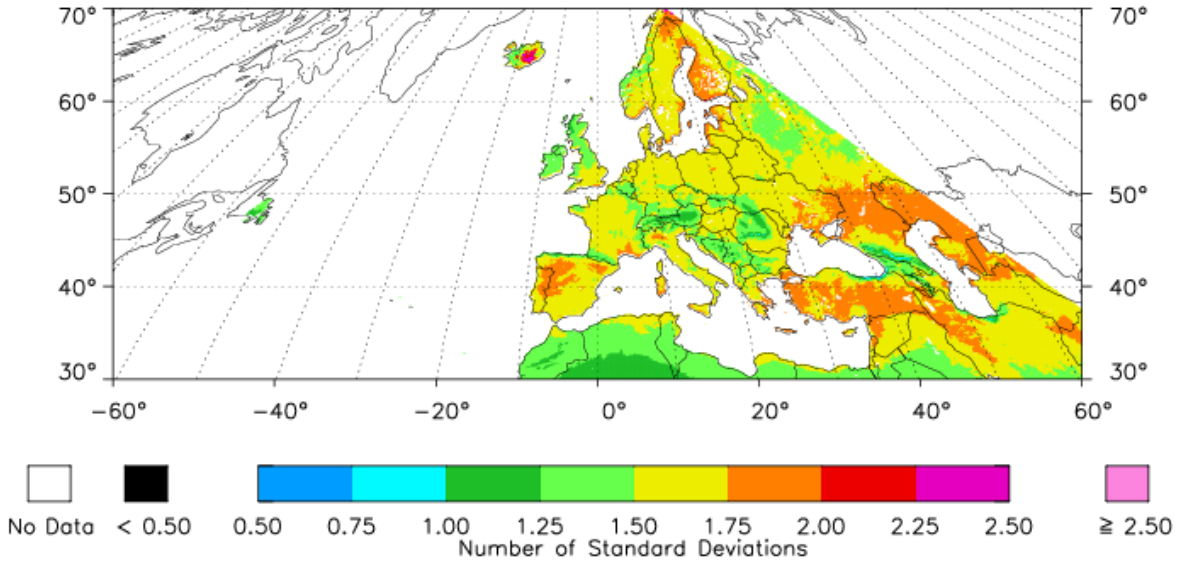


Figure 6: EOF-1 of annual cycle of surface incoming shortwave flux SIS.

The map of EOF-1 for incoming shortwave SIS describes the geographical distribution corresponding to PC-1 and is shown by Figure 6. EOF-1 is small at low latitudes and increases with latitude, as does the annual cycle of TOA insolation, but there are strong longitudinal variations, which are attributed to clouds. If clouds increase in summer as compared to winter, EOF-1 for SIS is decreased and vice versa for increased

winter cloudiness. Thus, over Asia Minor EOF-1 is large, indicating that in summer the cloudiness is less than in winter. For Austria and Bavaria, the opposite occurs.

Figure 7 shows the principal components of surface net shortwave SNS. These are very similar to those for SIS, except diminished. The surface net shortwave SNS is the heating term for the surface.

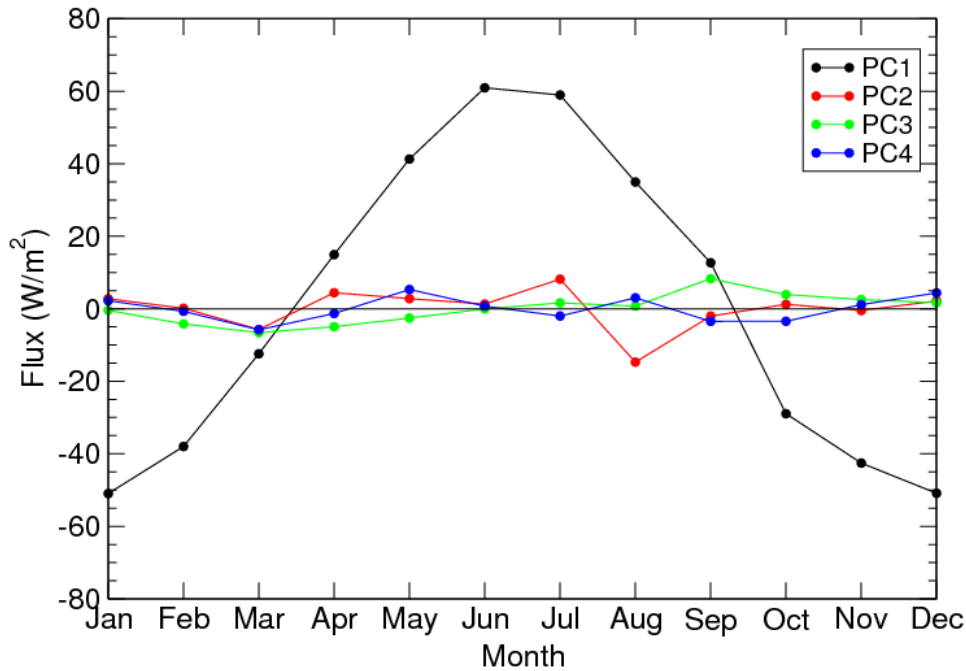


Figure 7: Principal components of the annual cycle of surface net shortwave flux SNS.

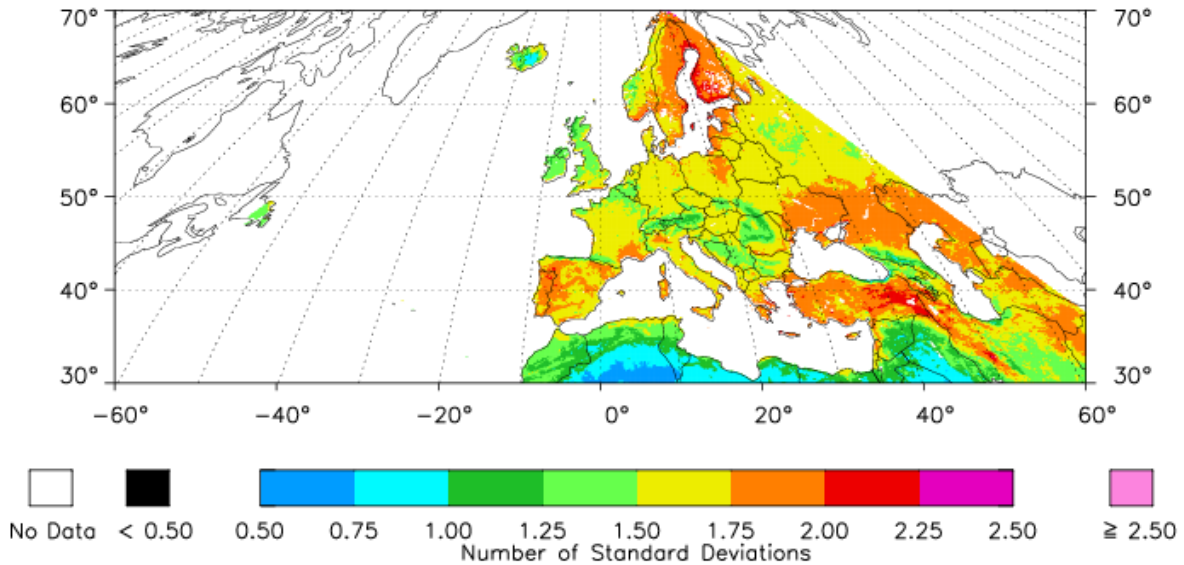


Figure 8: EOF-1 of annual cycle of surface net shortwave flux SNS.

Figure 8 shows EOF-1 for SNS. The Scandinavian Peninsula has somewhat higher values than it does for EOF-1 of the incoming shortwave SIS. This is perhaps due to snow cover in the winter. There are smaller net shortwave values over snow because much of the incoming shortwave radiation is reflected back. This would deepen the winter portion of the annual cycle of net shortwave in these areas, making the values of SNS lower and thereby increasing the EOF-1 values.

The surface net shortwave flux SNS heats the surface, causing the surface temperature and thus surface outgoing longwave radiation SOL to change. Figure 9 shows the principal components for SOL. The surface emissivity is assumed to be 1.0, so that SOL is simply the blackbody radiation for the surface temperature. PC-1 for SOL is a sine wave with its maximum in July, whereas the SNS had its maximum in June. Also, the PC-1 for SIS was asymmetric, but PC-1 for SOL is quite symmetric. The amplitude for PC-1 of SOL is very near $\pm 50 \text{ W m}^{-2}$, as for PC-1 of SNS. The variance explained by PC-2 of SOL is only 2.1% of the variance of SOL, so that its amplitude shown in fig. 9 is small, only reaching 10 W m^{-2} at its peak and valley, and the higher order terms are even smaller.

Figure 10 is a map of EOF-1 of the annual cycle of surface outgoing longwave radiation SOL. The annual cycle of SOL is small for Iceland, Ireland and Scotland, quantifying the effect of the ocean on ameliorating the climate of these areas. The remainder of Great Britain as well as the Normandy coast of France have EOF-1 values near 1. Inland, western Europe and the coast of North Africa have slightly higher values. To the east, EOF-1 for the annual cycle of SOL has values of 1.5 and greater, demonstrating a large longitudinal effect on SOL.

The atmosphere heats in response to the surface heating, so that the downward longwave radiation SDL at the surface varies as shown by its principal components in fig. 11. PC-1 is a sine wave, with range of $\pm 35 \text{ W m}^{-2}$ and maximum very near that of SOL. PC-2 has a sharp maximum of 10 W m^{-2} in December and a broad minimum from February to May of -5 to -7 W m^{-2} . The effect of PC-2 is to shift the onset of spring in regions where EOF-2 is large.

The geographical distribution of EOF-1 of surface downward longwave flux SDL is shown by fig. 12. This map is very similar to that for SOL, which may be due to the close coupling between SOL and SDL.

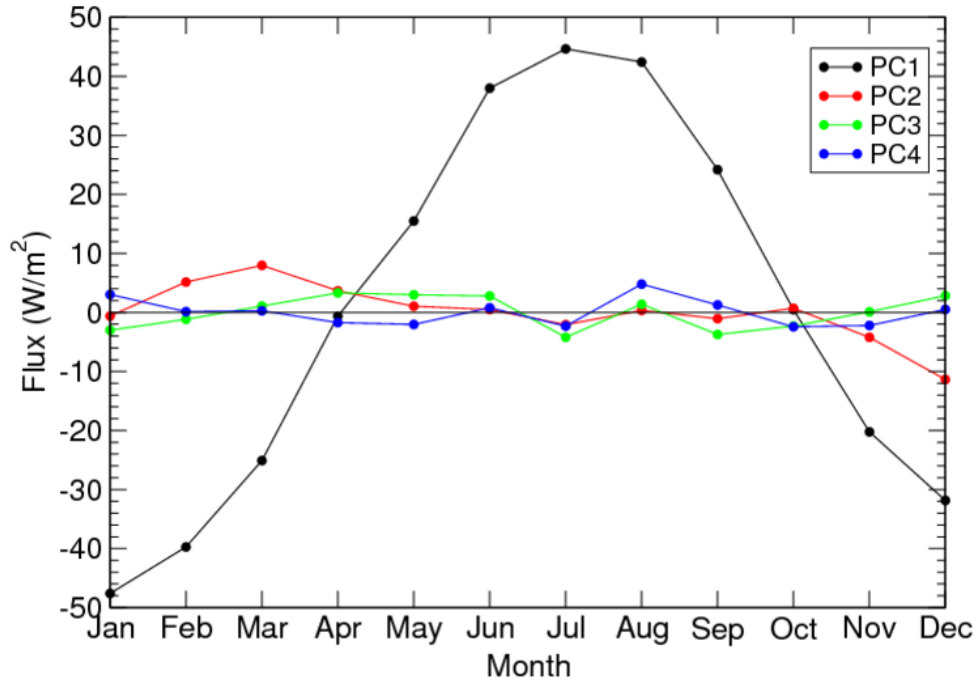


Figure 9: Principal components of the annual cycle of surface outgoing longwave flux SOL.

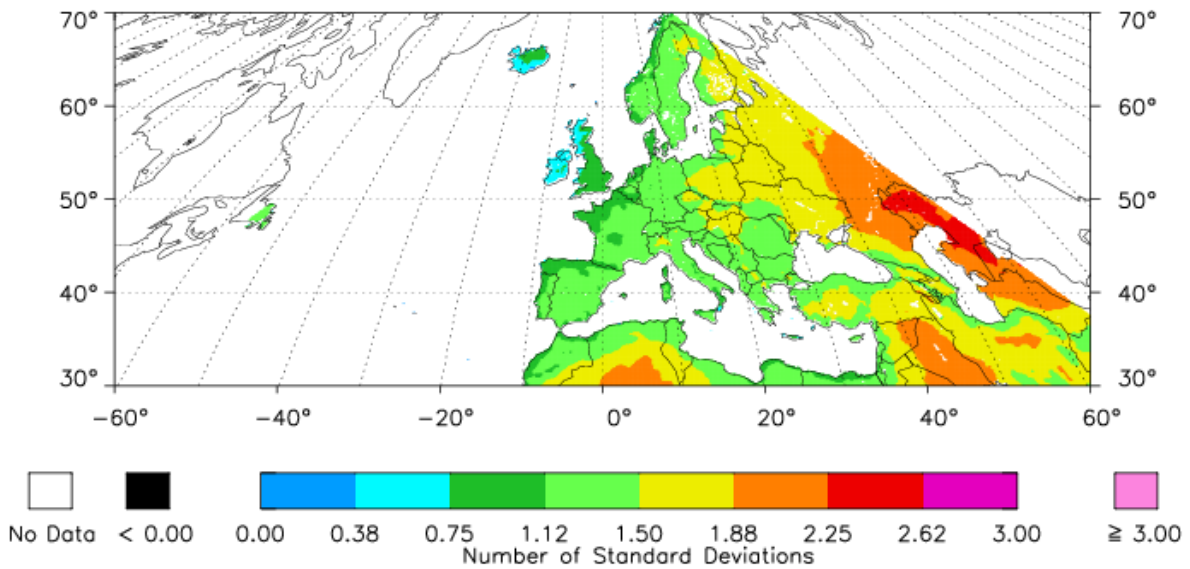


Figure 10: EOF-1 of annual cycle of surface outgoing longwave flux SOL.

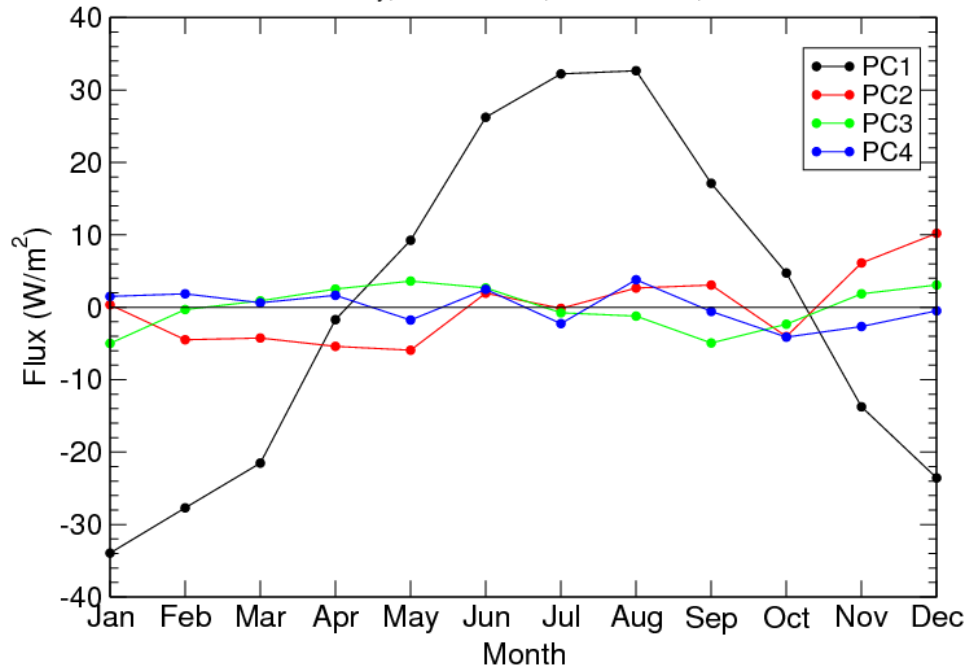


Figure 11: Principal components of the annual cycle of surface downward longwave flux SDL.

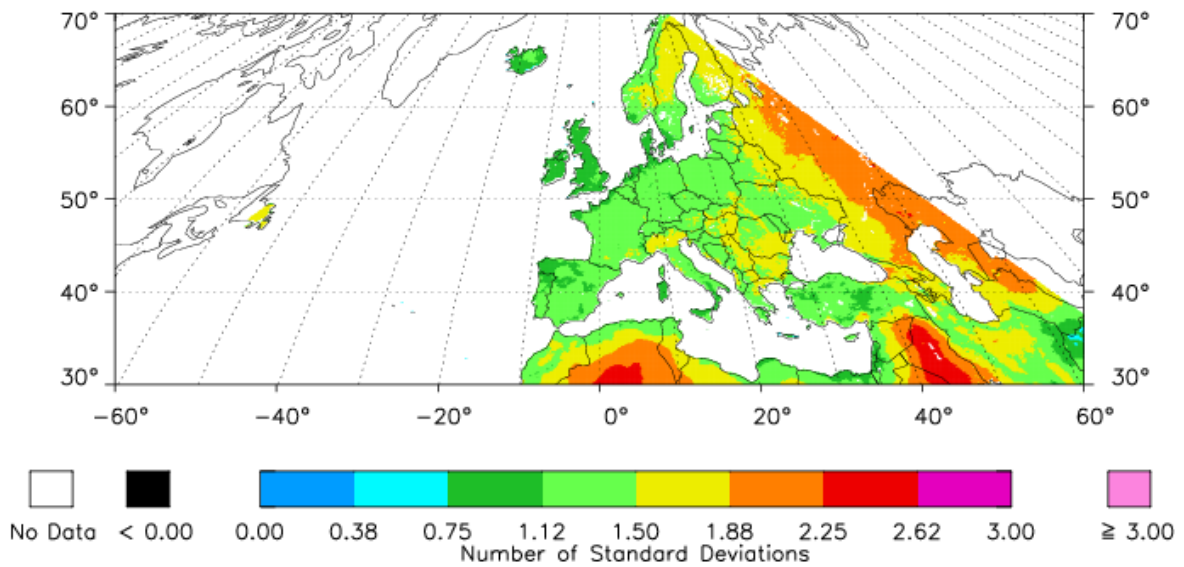


Figure 12: EOF-1 of the annual cycle of surface downward longwave flux SDL.

The shortwave net and longwave net fluxes are added together to give the surface total net radiation flux. The total net flux provides the heating/cooling of the surface which goes into sensible and latent heat at the lower boundary of the atmosphere. Table 1 shows that for the total net flux, 96% of the variance is described by the first principal component PC-1 and 1% by PC-2. Figure 13 shows the first four principal components of total net flux. PC-1 is close to a

sine wave with maximum and minimum at the solstice months of June and December and a range of $+50$ to -40 W m^{-2} .

Figure 14 is a map of EOF-1 of total net flux. The annual cycle is surprisingly uniform over much of western Europe. The latitudinal and longitudinal variations which were noted in the other components of surface radiation are not as evident in the total net flux.

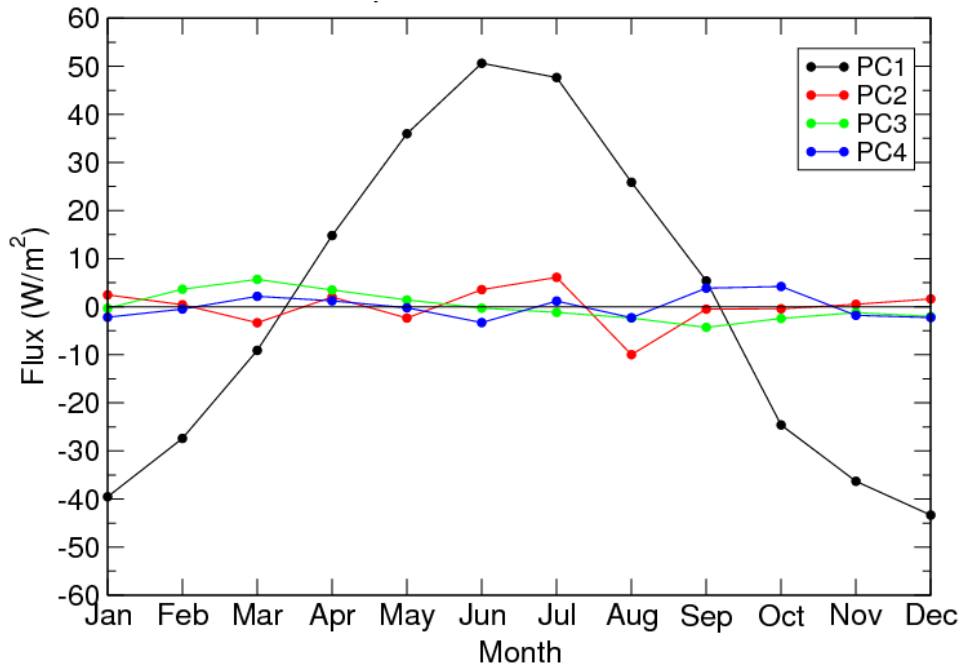


Figure 13: Principal components of the annual cycle of surface total net flux.

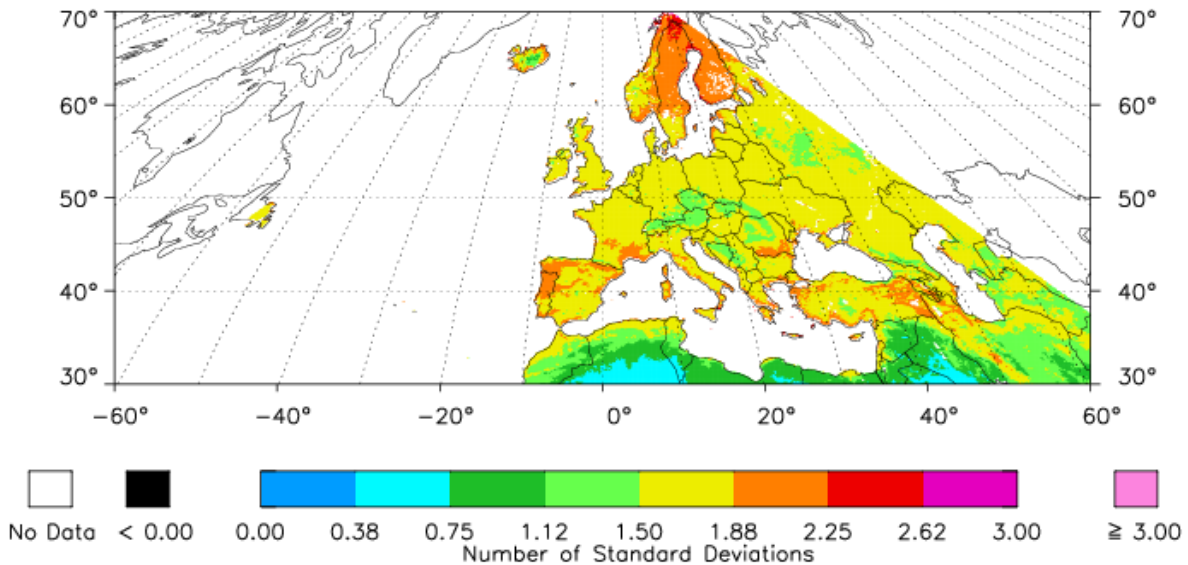


Figure 14: EOF-1 of the annual cycle of surface total net flux.

5. DISCUSSION

The longitudinal variations noted were frequently attributed to clouds. Further investigation is required to verify that clouds are the cause of these variations. Likewise, the strong changes of EOF-1 for surface net shortwave SNS over the Scandinavian Peninsula were presumed to be due to snow cover. Whether this is the case or not needs to be verified.

Examination of the various EOF maps in this paper shows small features which can be resolved by the fine scale of the data set. These features are largely due to mountains or proximity to coasts. This resolution may permit studies of the surface radiation budget at the mesoscale level.

6. CONCLUSIONS

The Surface Radiation Budget data set developed by the Climate Monitoring Satellite Applications Facility has been used to examine the annual cycle of SRB components over the European sector at 15 km resolution for January 2006 through December 2006. Annual mean maps of shortwave and longwave components have strong longitudinal variations, largely due to cloud forcing. The annual variations of shortwave and longwave radiation are primarily due to a single annual cycle term, with small effects due to the out-of-phase annual cycle and semi-annual cycle terms. The annual cycles of shortwave and longwave have strong longitudinal variations, which are attributed to cloud forcing. The total net radiation flux is quite uniform over western Europe.

Acknowledgements: PEM and GLS were supported by the Earth Science Office of NASA through the Surface Radiation Budget Project in the Science Directorate of Langley Research Centre. RH is supported by the German Meteorological Service. Data sets were provided by the German Meteorological Service.